A high-performance multi-wavelength optical switch based on multiple Fano resonances in an all-dielectric metastructure[*]

CAO Shuangshuang[1], FAN Xinye[1,2,3,4**], FANG Wenjing[1,2,3], CHEN Huawei[1], BAI Chenglin[1,2,3], and TONG Cunzhu[5**]

1. *School of Physics Science and Information Engineering, Liaocheng University, Liaocheng 252000, China*
2. *Shandong Provincial Key Laboratory of Optical Communication Science and Technology, Liaocheng 252000, China*
3. *Liaocheng Key Laboratory of Industrial-Internet Research and Application, Liaocheng 252000, China*
4. *Institute of Semiconductors, Chinese Academy of Sciences, Beijing 100083, China*
5. *State Key Laboratory of Luminescence and Applications, Changchun Institute of Optics, Fine Mechanics and Physics, Chinese Academy of Sciences, Changchun 130033, China*

The multi-wavelength optical switch based on an all-dielectric metastructure consisting of four asymmetric semi-circular rings was designed and analyzed in this paper. Four Fano resonance modes, which can be explained by bound states in the continuum (BIC) theory, are excited in our structure with a maximum Q-factor of about 2 450 and a modulation depth close to 100%. By changing the polarization direction of the incident light, the transmission amplitude of Fano resonances can get effectively modulated. Based on this tuning property, the metastructure can achieve a multi-wavelength optical switch in the near-infrared region (900—980 nm) and the maximum extinction ratio can reach 38.3 dB. In addition, the results indicate that the Fano resonances are sensitive to the changes in the refractive index. The sensitivity (S) and the figure of merit (FOM) are 197 nm/RIU and 492 RIU^{-1}. The proposed metastructure has promising potential in applications such as optical switches, sensors, modulators and lasers.

Document code: A **Article ID:** 1673-1905(2024)04-0193-7

DOI https://doi.org/10.1007/s11801-024-3147-9

The optical switch is a device that can operate at one or multiple wavelengths for the physical switch or logical operation of optical signals in optoelectronic integrated circuits. Different types of optical switches can be implemented on the basis of various physical mechanisms, such as electro-optical effect[1], thermo-optical effect[2], all-optical response[3], and so on, characterized by the response time, compactness and low energy consumption. However, it is rare for these optical switches to achieve at multiple wavelengths simultaneously. Multiple Fano resonances can be exploited to achieve multi-wavelength optical switches as the transmission amplitude of Fano resonances can get effectively modulated by the polarization direction of the incident light[4], which provides a promising approach to achieving multi-wavelength optical switches.

Fano resonance is an asymmetric spectral lineshape phenomenon caused by the destruction of interference between continuous and discrete local states, which can be excited in metastructures[5,6]. An efficient approach to achieving high Q-factor Fano resonance is on the basis of bound states in the continuum (BIC) in all-dielectric metastructures[7,8]. However, the ideal BIC is a mathematical model, which is not applicable to optical devices due to the characteristics of an exceptionally thin linewidth and an infinitely high Q-factor[9,10]. By breaking the symmetry of metastructures, the radiation channel with the outside can be established, which allows the ideal BIC is disturbed and converted to a quasi-BIC mode, leading to limited linewidth and Q-factor[11,12]. The high Q-factor Fano resonance makes the optical switch possess precise control of a single wavelength, which is necessary for optical switch or detection. Therefore, it is meaningful to design a metastructure that excites multiple Fano resonances with excellent properties, such as high Q-factor and high modulation depth.

The optical switches based on an all-dielectric metastructure can be achieved by altering the polarization direction of the incident light[13-15]. For example, LI et al[16] presented a single-wavelength optical switch based on an all-dielectric metastructure composed of two square air holes. WANG et al[17] presented a multi-wavelength optical switch based on an all-dielectric metastructure consisting of permittivity-asymmetric rectangular holes, but the extinction ratio was not sufficiently high. The optical switch is used as a critical device, the greater the number of switching wavelengths simultaneously, the stronger the ability of communication and processing[18]. However, the performance of the optical switch is hindered by operating at a single wavelength or having a low extinction ratio. Therefore, it is still a challenge to achieve high-performance multi-wavelength optical switches.

In this paper, the multi-wavelength optical switch based on an all-dielectric metastructure was designed over the wavelength range of 900—980 nm. The metastructure consists of four semi-circular rings periodically placed on a SiO_2 substrate, which can excite multiple Fano resonances with excellent performance. By changing the geometric parameters of structure, the Fano resonances can be adjusted to make it more appropriate for prospective applications. The results show that the structure can be applied as a multi-wavelength optical switch and a multi-channel refractive index sensor. In particular, the optical switch can simultaneously achieve on and off states at four different wavelengths. Therefore, the designed metastructure can be used as optical switches, sensors and modulators.

Fig.1 shows the schematic diagram of the designed optical switch based on the metastructure laid on a SiO_2 substrate, which consists of four semi-circular rings. In Fig.1(b), the outer and inner radii of the semi-circular rings are R and r_1 (r_2), respectively. The asymmetry parameter Δr is defined as $\Delta r=r_1-r_2$. The depth of semi-circular ring is H and the center point of the structure is d from the center of semi-circular ring. The periods are respectively P_x and P_y in the x and y directions. The finite-difference time-domain (FDTD) method is adopted to simulate and analyze the optical properties of the designed structure. In x and y directions, the periodic boundary conditions are set as well as the perfectly matched layers (PML) boundary conditions are used in the z direction. In Fig.1(a), there exists the electric field of the plane wave is x-polarized (polarization angle $\theta=0°$), while the wave vector is propagating in the z direction. Here θ is the angle between the x-axis and the polarization direction of the electric field. In addition, the material characteristics of Si and SiO_2 are obtained from the Palik handbook[19].

Fig.2 shows the calculated transmission spectra of the designed structure at different asymmetric parameters when $P_x=P_y$=730 nm, H=150 nm, d=150 nm, R=150 nm. When Δr=0 nm ($r_1=r_2$=80 nm), one sharp Fano resonance appears at λ=959.7 nm (P1'). If Δr=30 nm

(r_1=80 nm, r_2=50 nm), the symmetry of the structure is disrupted due to the difference between r_1 and r_2, establishing a radiation channel between the free space continuum and the non-radiative bound state. Three new Fano resonances appear at λ=911.1 nm (P1), λ=930.2 nm (P2) and λ=973.3 nm (P4), respectively. However, comparing with Δr=0 nm, the P1' peak shifts to 962.0 nm (P3) and the linewidth of P1' peak becomes wider, which shows the break in structural symmetry causes a wider radiation channel at the P1' peak, leading to the leakage of radiative energy and a corresponding reduction in the Q-factor.
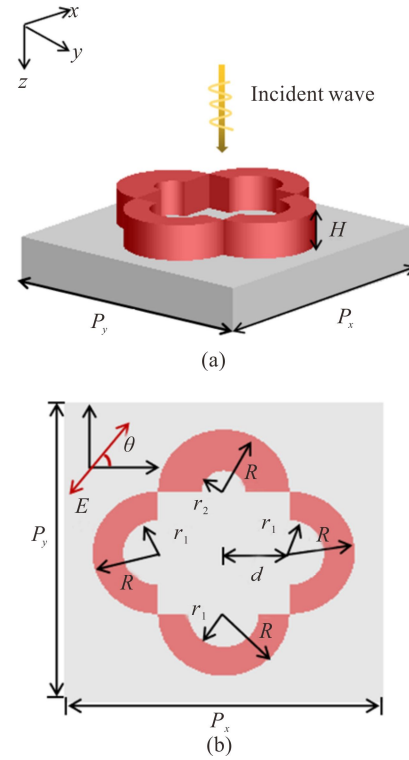

Fig.1 Schematic diagram of the designed optical switch based on the metastructure: (a) The metastructure of a single unit cell laid on a SiO_2 substrate and consisting of four semi-circular rings; (b) The geometrical parameters are defined as $\Delta r=r_1-r_2$, $P_x=P_y$=730 nm, H=150 nm, R=150 nm, and d=150 nm
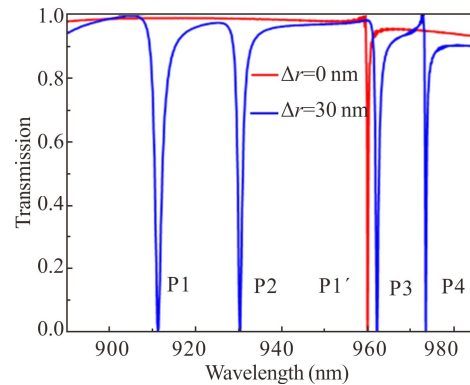

Fig.2 Transmission spectra of the designed structure at different asymmetry parameters

The performance of the Fano resonance can be evaluated by Q-factor and modulation depth. The modulation depth ΔT is denoted as[20]

$$\Delta T = T_{peak} - T_{dip}, \tag{1}$$

which represents the difference between the transmission amplitudes of the Fano resonance at the peak and dip. The modulation depth at the P1 and P4 resonances can approach 100%, as well as 97.5% and 98.5% at P2 and P3 resonances, respectively. In addition, the Fano resonance waveform in the transmission spectra is usually represented by the following function[21]

$$T = \left| a_1 + ia_2 + \frac{b}{\omega - \omega_0 + i\gamma} \right|^2, \tag{2}$$

in which a_1, a_2 and b are defined as real constants, γ and ω_0 respectively are the overall damping loss and the resonant frequency. Fig.3(a) shows the fitting transmission spectra of the P1'. It is obvious that the fitting curve agrees with the simulation curve. Furthermore, the Q-factor of the Fano resonance is calculated by[22]

$$Q = \omega_0/2\gamma. \tag{3}$$

The Q-factors of P1, P2, P3, and P4 resonances are respectively around 512, 788, 1 205, and 2 450, when $\Delta r = 30$ nm. Fig.3(b) presents the dependent relationship between the Q-factors of four Fano resonances and the asymmetry parameter Δr. It can be found that the Q-factors become smaller as asymmetry parameter Δr increases. This is because that the radiation channel becomes wider as the asymmetry parameter Δr becomes larger, resulting in more energy being radiated into the free space and a decrease in Q-factor. Therefore, multiple Fano resonances can be excited in the designed metastructure and these Fano resonances show the great characteristics of high modulation depth and high Q-factor.

To investigate the physical mechanism of each Fano resonance, the electromagnetic field distributions at respective resonances for $\Delta r = 30$ nm are simulated in Fig.4. At the P1 resonance mode, two reversed magnetic field arrows are formed along the y direction in the y-z plane. In the x-y plane, the magnetic field forms four magnetic loop currents, which results in a magnetic quadrupole (MQ) resonance mode. For the resonance mode at P2, a current circle is generated in the x-y plane, and an arrow along the z direction is formed in the y-z plane, indicating a magnetic dipole (MD) resonance mode oscillating along the z direction. For P3 resonance mode, two loops with opposite directions are generated in the x-y plane. Meanwhile, the magnetic field creates two reversed arrows in the y-z plane to form a clockwise loop, indicating a toroidal dipole (TD) resonance mode along the x-negative direction. According to the current distributions in the x-y plane and two opposite loops formed in the y-z plane, which indicate an electric quadrupole (EQ) resonance mode at P4 resonance.
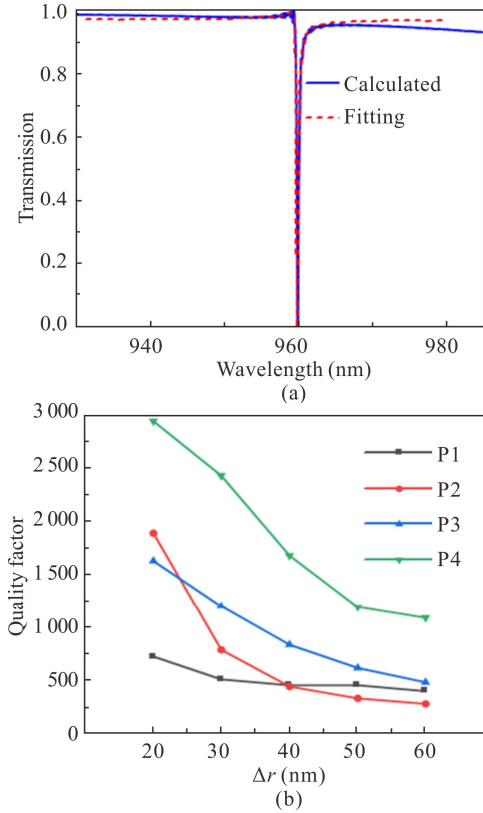

(a)

(b)

Fig.3 (a) The fitting result of P1'; (b) The dependent relationship between the Q-factors of four Fano resonances and the asymmetry parameter Δr

Further, the transmission spectra with different geometric parameters for the asymmetric parameter $\Delta r = 30$ nm are shown in Fig.5. It can be seen that four resonance peaks generate a significant red shift as the structure period increases from 715 nm to 745 nm. In Fig.5(b), it is clear that four resonance peaks have a red shift as the thickness of four semi-circular rings changes from 230 nm to 250 nm. This is attributed to the increase in effective refractive index of the metastructure with the increase of thickness. As illustrated in Fig.5(c), the P1
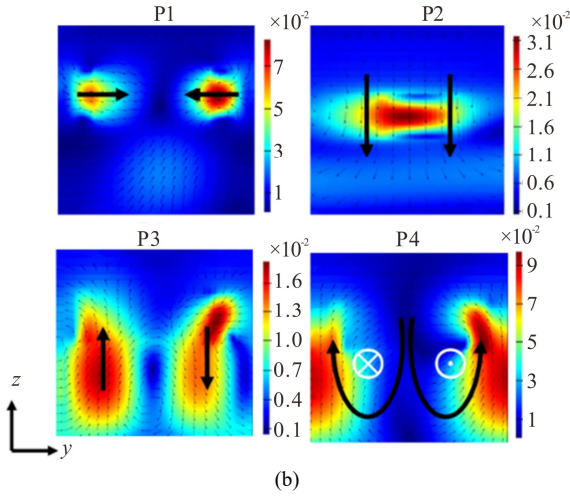

(a)
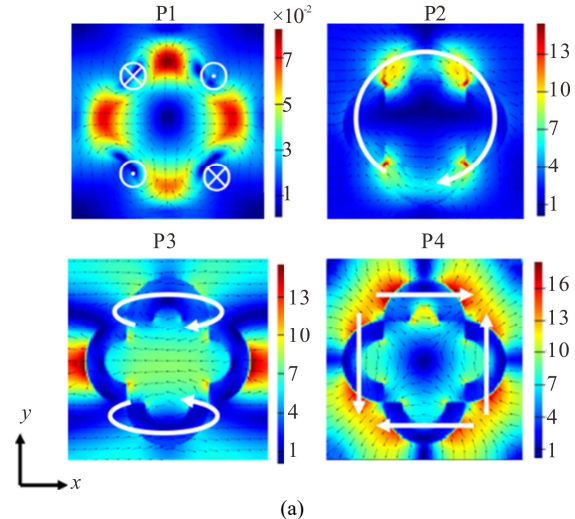
Fig.4 When Δ*r*=30 nm, electromagnetic field distributions at the corresponding resonance peaks: (a) The color maps at P2, P3 and P4 (P1) resonance modes denote *E_z* (*H_z*) distributions (Small black arrows represent the distributions of electric (magnetic) field vectors at P2, P3 and P4 (P1) resonant modes and white arrows denote the electric field directions); (b) The color maps denote respective magnetic field amplitudes |*H*/*H_0*| and black arrows indicate the magnetic field directions

and P2 resonances generate a distinct red shift as the outer radius *R* increases from 145 nm to 155 nm, while P3 and P4 resonances have a slight red shift compared to P1 and P2 resonances. In Fig.5(d), four resonance peaks have an obvious red shift as the asymmetry parameter Δ*r* increases from 20 nm to 40 nm. Meanwhile, the linewidth of four resonance peaks becomes wider with increasing asymmetry parameter Δ*r*, leading to a significant decrease in the Q-factor of resonances. As a result, multiple Fano resonances have good tunability by adjusting the geometric parameters.

In addition, the transmission spectra of the structure placed in an environment with different refractive indexes are analyzed in Fig.6. In Fig.6(a)—(c), the four resonance peaks have a clear red shift when the structure is laid in an environment as the refractive index changes from 1.0 to 1.05. Fig.6(d) shows the corresponding linear fitting of the relationship between the resonant wavelength offset and the various refractive indexes of P1, P2, P3 and P4 resonance peaks. The fitting degrees are 0.999 55, 0.999 21, 0.998 5, and 0.998 0, respectively, exhibiting good linear responses. In addition, the sensitivity is defined as[12]

$$S = \frac{\Delta\lambda}{\Delta n},$$ (4)

where Δ*λ* and Δ*n* represent the resonant wavelength offset and refractive index difference, respectively. The figure of merit (*FOM*) can be obtained using[12]
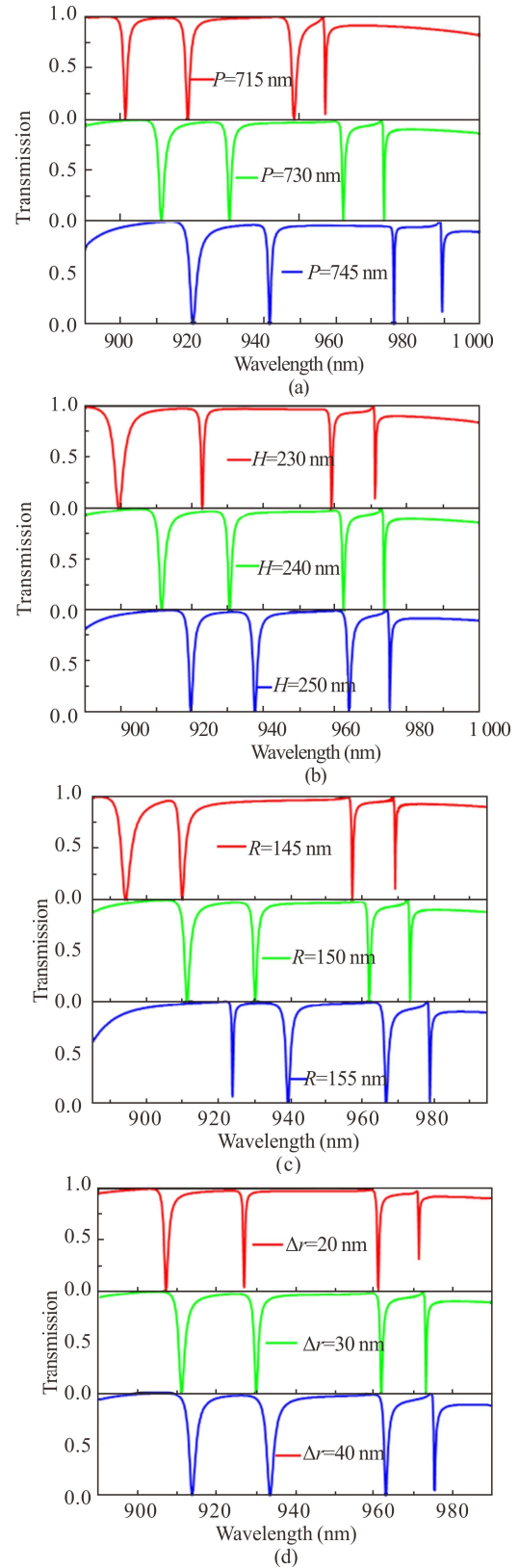
$$FOM = \frac{S}{FWHM},$$ (5)

Fig.5 Transmission spectra of the designed structure with different geometric parameters: (a) Period *P*; (b) Thickness *H*; (c) Outer radius *R*; (d) Asymmetry parameters Δ*r*

which is the ratio between sensitivity (*S*) and the full width at half maximum (*FWHM*). The *S* of P1, P2, P3

and P4 resonance peaks can reach 114 nm/RIU, 104 nm/RIU, 176 nm/RIU and 197 nm/RIU, and the respective *FOMs* are about 64 RIU^{-1}, 88 RIU^{-1}, 220 RIU^{-1} and 492 RIU^{-1}, respectively. These results show that Fano resonances are sensible to changes in the refractive index of the environment, which can be applied to achieve a sensor with high performance.

The proposed metastructure can be used as a multi-wavelength optical switch. The transmission spectra at different polarization directions when the asymmetry parameter $\Delta r=30$ nm are shown in Fig.7. To analyze the switching characteristics of the metastructure, the extinction ratio (*EXT*) and the value of transmission amplitude difference ΔT_1 are defined as[23]

$$EXT=10\log_{10}(T_{on}/T_{off}) \tag{6}$$

$$\Delta T_1=T_{on}-T_{off}, \tag{7}$$
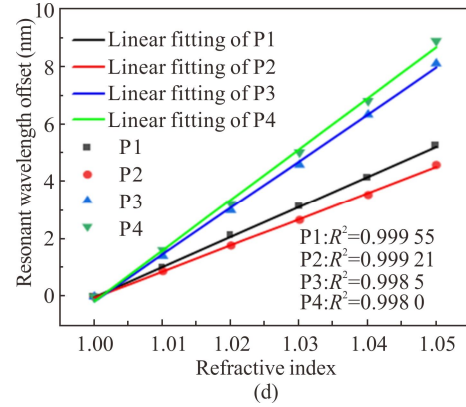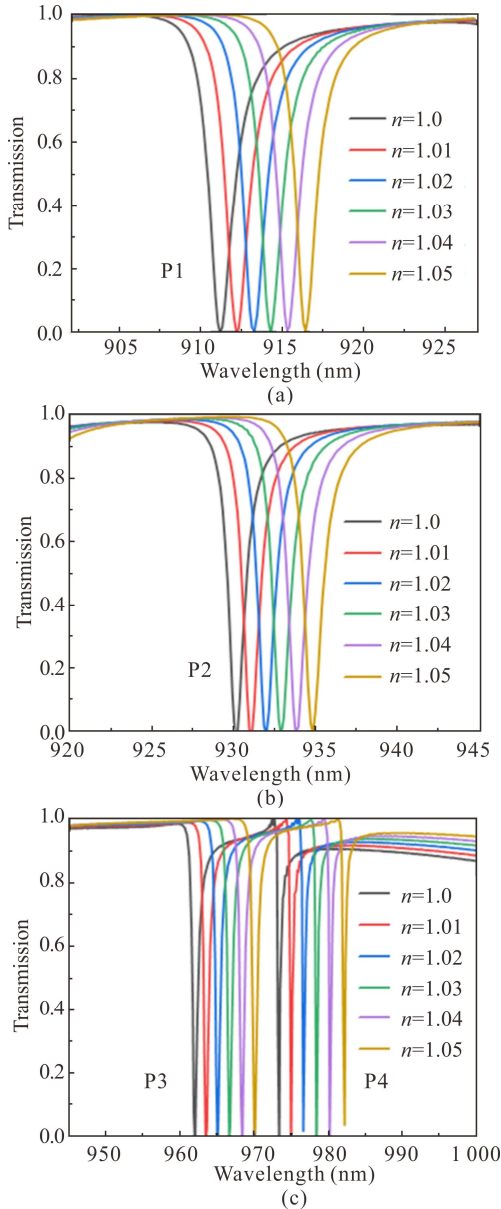

(a)

(b)

(c)

(d)

Fig.6 Transmission spectra of the structure placed in an environment with different refractive indexes for (a) P1, (b) P2 and (c) P3 and P4; (d) Linear fitting of the relationship between the resonant wavelength offset and the various refractive indexes of P1, P2, P3 and P4 resonance peaks

where T_{on} and T_{off} represent the maximum and minimum transmission amplitudes, respectively. In Fig.7(a)—(c), as the polarization angle θ increases, the P1, P2, P3, and P4 resonance peaks gradually disappear, while two new resonances appear, called P5 and P6 here. The results indicate that Fano resonance peaks are polarization-dependent and can be excited at the specific polarization direction of the incident light.

The variation of transmission amplitudes as the polarization angle changes from 0° to 90° at each resonance peak are shown in Fig.7(d). It is obvious that the transmission amplitudes of P1, P2, P3 and P4 resonance peaks gradually increase, while the transmission amplitudes of P5 and P6 resonance peaks show a decreasing trend. The values of transmission amplitude difference of P1—P6 resonance peaks are 98.92%, 99.17%, 98.01%, 96.73%, 73.13%, and 51.59%, respectively. Particularly, the transmission amplitudes of P1, P2, P3, P4 can be modulated from 0 to roughly 100% without obvious wavelength shifts, indicating a complete switching effect. The extinction ratio of P1, P2, P3, P4, P5, and P6 resonances can reach about 31.1 dB, 26.9 dB, 25.1 dB, 38.3 dB, 6.1 dB, and 4.6 dB, respectively. Considering the optical switch need to meet a certain transmission amplitude difference and extinction ratio in practical applications, this structure can achieve an optical switch with excellent performance at four different wavelengths. In addition, the proposed multi-wavelength optical switch based on an all-dielectric metastructure shows better performance comparing with the plasmonic metastructure optical switches[24,25].

The number and transmission amplitude difference ΔT_1 calculated in this paper are compared with the prepared works in the references. As shown in Tab.1, it can be observed that the proposed structure achieves a high performance for the multi-wavelength optical switch.
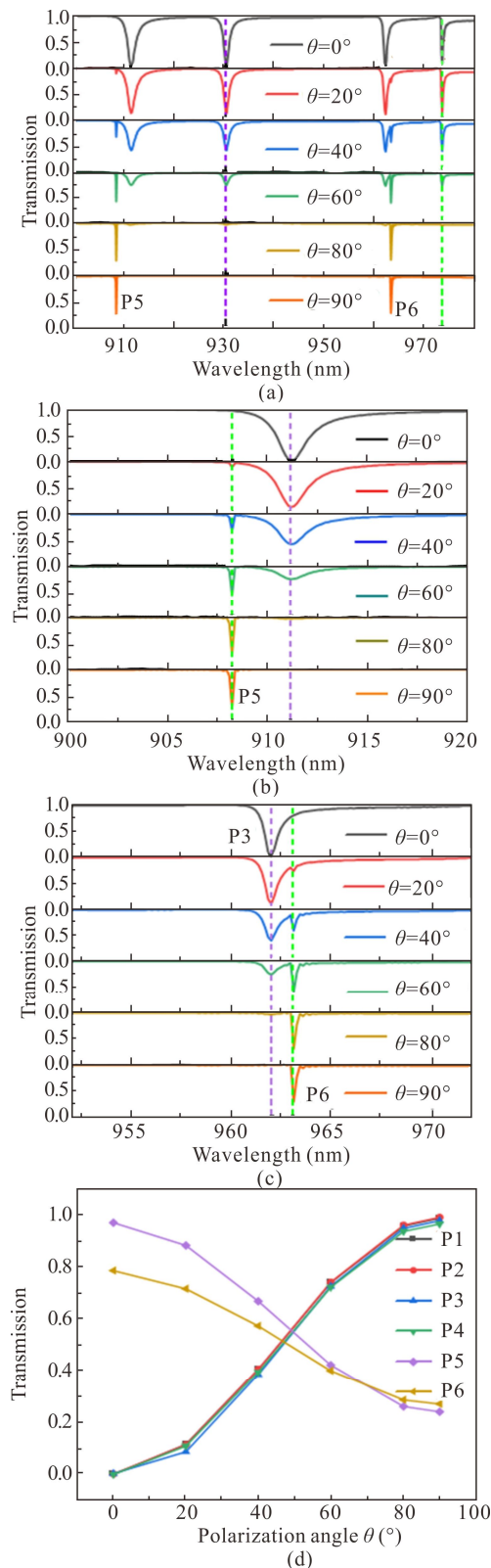
Fig.7 (a) Transmission spectra at different polarization directions; (b) Transmission spectra of P1 and P5 resonance peaks at different polarization directions; (c) Transmission spectra of P3 and P6 resonance peaks at different polarization directions; (d) The variations of transmission amplitudes as the polarization angle changes from 0° to 90° at each resonance peak

Tab.1 Comparison of performance

Optical switch type	Number	ΔT_1
Rhombus all-dielectric metasurface[5]	4	98%
		50%
		93%
		80%
Asymmetric cross metasurface[15]	2	95%
		85%
Permittivity-asymmetric dielectric metasurface[17]	3	85%
		85%
		80%
A rectangular like tetramer structure[23]	2	84.39%
		84.23%
This work	4	98.92%
		99.17%
		98.01%
		96.73%

In summary, the multi-wavelength optical switch based on an all-dielectric metastructure that consists of semi-circular rings was proposed. By breaking the symmetry of the structure, four sharp Fano resonances are excited, where the maximal Q-factor can reach 2 450 and relative resonance modes are MQ, MD, TD and EQ, respectively. The optical switch is obtained by varying the polarization direction of the incident light. Particularly, the transmission amplitudes at four Fano resonances can be modulated from 0 to roughly 100% and the maximum extinction ratio can reach 38.3 dB. In addition, the S and FOM reach about 197 nm/RIU and 492 RIU^{-1}, which indicate the structure can be used as a sensor due to its sensitivity to the refractive index in the environment. The proposed metastructure has extensive applications in optical switches, sensors and modulators due to the Fano resonances with high Q-factor and high modulation depth.

Ethics declarations

Conflicts of interest

The authors declare no conflict of interest.

References

[1]   CHEN Y K, WANG Y. Electrically tunable toroidal Fano resonances of symmetry-breaking dielectric metasurfaces using graphene in the infrared region[J]. Journal of optics, 2022, 24(4): 044012.

[2]   JIANG H, HAN Z H. Spectral stability of bound state in the continuum resonances due to thermal effect and the application as efficient thermo-optic modulators[J]. Optics communications, 2022, 515: 128216.

[3]   HAN Z H, CAI Y J. All-optical self-switching with ultralow incident laser intensity assisted by a bound

state in the continuum[J]. Optics letters, 2021, 46(3): 524-527.

[4]   XING J J, LI H, YU S L, et al. Multiple Fano resonances driven by bound states in the continuum in an all-dielectric nanoarrays system[J]. AIP advances, 2023, 13(3): 035212.

[5]   YE Y C, YU S L, LI H, et al. Triple Fano resonances metasurface and its extension for multi-channel ultra-narrow band absorber[J]. Results in physics, 2022, 42: 106025.

[6]   ZHANG Y B, LIU W W, LI Z C, et al. High-quality-factor multiple Fano resonances for refractive index sensing[J]. Optics letters, 2018, 43(8): 1842-1845.

[7]   FAN K, SHADRIVOV I V, PADILLA W J. Dynamic bound states in the continuum[J]. Optica, 2019, 6(2): 169-173.

[8]   GARMON S, NOBA K, ORDONEZ G, et al. Non-Markovian dynamics revealed at a bound state in the continuum[J]. Physical review A, 2019, 99(1): 010102.

[9]   ZHAO H N, FAN X Y, WEI X, et al. All-dielectric metastructure based on multiple Fano resonances with high sensitivity[J]. Optics communications, 2023, 530: 129193.

[10]   YU S L, LI H, WANG Y S, et al. Multiple Fano resonance excitation of all-dielectric nanoholes cuboid arrays in near infrared region[J]. Results in physics, 2021, 28: 104569.

[11]   YANG L, YU S L, LI H, et al. Multiple Fano resonances excitation on all-dielectric nanohole arrays metasurfaces[J]. Optics express, 2021, 29(10): 14905-14916.

[12]   BI L P, FAN X Y, LI C C, et al. Multiple Fano resonances on the metastructure of all-dielectric nanopore arrays excited by breaking two-different-dimensional symmetries[J]. Heliyon, 2023, 9(1): e12990.

[13]   WANG D D, FAN X Y, FANG W J, et al. Excitation of multiple Fano resonances on all-dielectric nanoparticle arrays[J]. Optics express, 2023, 31(6): 10805-10819.

[14]   SHI Y, YU S L, LI H, et al. Ultra-high quality factor resonances in a pinwheel-shaped all-dielectric metasurface

based on bound states in the continuum[J]. IEEE photonics journal, 2023, 15(2): 1-7.

[15]   FAN H J, LI J, SUN Y H, et al. Asymmetric cross metasurfaces with multiple resonances governed by bound states in the continuum[J]. Materials, 2023, 16(6): 2227.

[16]   LI H, YU S L, YANG L, et al. High Q-factor multi-Fano resonances in all-dielectric double square hollow metamaterials[J]. Optics and laser technology, 2021, 140: 107072.

[17]   WANG Y S, HU Z H, ZHAO T G, et al. High Q-factor Fano resonances on permittivity-asymmetric dielectric meta-surfaces[C]//Proceedings of Nanophotonics and Micro/Nano Optics VII, October 10-12, 2021, Nantong, China. New York: SPIE, 2021, 11903: 139-145.

[18]   JIANG X Q, BAO J L, SUN X D. Multiwavelength optical switch based on controlling the Fermi energy of graphene[J]. Physical review applied, 2018, 9(4): 044026.

[19]   PALIK E D. Handbook of optical constants of solids[M]. New York: Academic Press, 1985: 547-569.

[20]   WANG W D, ZHENG L, LIU Y J, et al. High-quality-factor multiple Fano resonances in free-standing all-dielectric nanodisk dimers for applications[J]. Optik, 2020, 207: 163815.

[21]   XU L, ZANGENEH K K, HUANG L J, et al. Dynamic nonlinear image tuning through magnetic dipole quasi-BIC ultrathin resonators[J]. Advanced science, 2019, 6(15): 1802119.

[22]   LI J, MA T. Magnetic toroidal dipole resonances with high quality factor in all-dielectric metamaterial[J]. Optics communications, 2022, 507: 127621.

[23]   NIU Q L, ZHU Y Q. Research on control of optical switch based on tetramer structure[J]. Transducer and microsystem technologies, 2023, 42(3): 40-44.

[24]   ZHANG L, DONG Z G, WANG Y M, et al. Dynamically configurable hybridization of plasmon modes in nanoring dimer arrays[J]. Nanoscale, 2015, 7(28): 12018-12022.

[25]   HE J N, WANG J Q, DING P, et al. Optical switching based on polarization tunable plasmon-induced transparency in disk/rod hybrid metasurfaces[J]. Plasmonics, 2015, 10: 1115-1121.